Journal of Power Sources 271 (2014) 167–173

Contents lists available at ScienceDirect

Journal of Power Sources

journal homepage: www.elsevier.com/locate/jpowsour

Electrochemical stability of aluminum current collector in alkyl carbonate electrolytes containing lithium bis(pentafluoroethylsulfonyl)imide for lithium-ion batteries

Seung-Taek Myung [a, b], Hitoshi Yashiro [b, *]

[a] Department of Nano Engineering, Sejong University, 98 Gunja-dong, Gwangjin-gu, Seoul 143-747, South Korea
[b] Department of Chemistry and Bioengineering, Iwate University, 4-3-5 Ueda, Morioka, Iwate 020-8551, Japan

HIGHLIGHTS

- Al foil passivates electrochemically in 1 M LiBETI in EC-DMC electrolyte.
- Al surface is passivated by a protective film: Al–F and Al–O(H) complexes.
- Li–Al alloy formation is significantly suppressed at 0 V versus Li/Li^+ during polarization.
- Al current collector is applicable in the range of 0.25–2 V, not forming Li–Al alloy.

ARTICLE INFO

Article history:
Received 25 April 2014
Received in revised form
13 July 2014
Accepted 15 July 2014
Available online 2 August 2014

Keywords:
Aluminum
Passivation
Current collector
Lithium
Battery

ABSTRACT

The electrochemical stability of aluminum in anhydrous alkyl carbonate electrolytes containing lithium bis(pentafluoroethylsulfonyl)imide (LiBETI, $LiN(SO_2C_2F_5)_2$), as compared with $LiPF_6$, has been investigated in terms of alloy formation with lithium at lower potentials (~0 V versus Li/Li^+) and repassivation of scratched surfaces at higher potentials (~5 V versus Li/Li^+), using cyclic and *in situ* scratch polarization tests and time-of-flight secondary ion mass spectroscopic (ToF-SIMS) analysis. Li–Al alloy formation at 0 V versus Li/Li^+ is significantly suppressed in a LiBETI electrolyte though it is common in a $LiPF_6$-containing electrolyte. ToF-SIMS analysis indicates that passive films on aluminum, which consist primarily of oxide/hydroxide, are less fluorinated in a LiBETI electrolyte than those formed in a $LiPF_6$ electrolyte. The less fluorinated oxide/hydroxide layer on aluminum is expected to be an important barrier against alloy formation in a LiBETI electrolyte. In combination with nano-sized SnO_2 powders, aluminum foil is successfully applicable as a current collector without Li–Al alloy formation in the range of 0.25–2 V versus Li/Li^+, although graphite electrodes do not operate properly in the same operation range. Thus, the large electrochemical stability of aluminum in LiBETI electrolyte makes it possible to be used as current collectors for both negative and positive electrodes.

1. Introduction

Aluminum is widely used as a current collector material for positive electrodes in commercial lithium-ion batteries because it meets most practical requirements including material cost, density, conductivity, malleability and corrosion stability. The corrosion stability of aluminum in typical electrolytes has been proven by many researchers [1–5]. Among the many electrolyte candidates for lithium-ion batteries, the $LiPF_6$-carbonate ester system is exclusively utilized. In the $LiPF_6$ system, aluminum is passivated, not only by oxide/hydroxide, but also by fluoride in the outer part [5]. It is generally understood that the outer fluoride layer plays an important role in the stability of aluminum against an HF attack when it is inevitably released from the decomposition of $LiPF_6$ salt, originating from the presence of a trace amount of water. Aluminum makes an alloy with electrochemically deposited lithium metal in the $LiPF_6$ system. Recently, we have reported that such alloy formation was strongly inhibited in a different electrolyte system: lithium bis-oxalato borate (LiBOB)-carbonate ester, which does not contain a halogen element [6]. In that system, aluminum is passivated only by oxide layers, which seem to be inert against electrochemical reduction, even at 0 V versus Li/Li^+

* Corresponding author. Tel.: +81 19 621 6330.
E-mail address: yashiro@iwate-u.ac.jp (H. Yashiro).

http://dx.doi.org/10.1016/j.jpowsour.2014.07.097
0378-7753/

(hereafter referred to as V). Hence, the relationship between the film structure on aluminum and its alloying behavior with lithium is an interesting matter to be further studied.

There is another promising electrolyte system for lithium-ion batteries: imide-based elctrolytes such as $LiN(SO_2CF_3)_2$ (LiTFSI) [7,8] and $LiN(SO_2C_2F_5)_2$ (LiBETI) [9,10]. These electrolytes are known to have good conductivity and durability against moisture and temperature. Although LiTFSI has high corrosiveness against aluminum, it can be inhibited by the addition of even small amounts of fluoroacid salts such as $LiPF_6$ [7] and $LiBF_4$ [8], or by less corrosive imides such as LiBETI [11]. According to Krause et al. [9], LiBETI induces thinner and denser films on aluminum compared to LiTFSI. The cycling behavior of a $LiCoO_2$/coke cell using a LiBETI electrolyte confirmed that there was no significant deterioration caused by aluminum corrosion, resulting in better performance than that using an $LiPF_6$ electrolyte [9,11].

Here in the present case, we are interested in the alloying behavior of aluminum with electrochemically deposited lithium in a LiBETI system because the passive films formed in a LiBETI electrolyte, which are possible barriers against alloying reactions, should differ from those in $LiPF_6$ and LiBOB electrolytes. In order to understand the alloying behavior, the passivation process of aluminum in a LiBETI electrolyte system should be also studied. Also, to understand the intrinsic stability of aluminum in a given electrolyte, the passivation process needs to be evaluated on a naked surface without air-formed oxide. One typical technique to remove an air-formed oxide layer is to polarize the surface to the potential range to a point where oxides can be reduced to metal. However, an oxide-free surface is not always yielded through the above treatment because every metal oxide is not electrochemically active. In that case, the remaining native layer can affect the alloying process as well as the apparent stability of passive films.

In the present work, preparation of new oxide-free metal surfaces is attempted using *in situ* mechanical scratches of aluminum surfaces that are polarized to given potentials to allow passivation or alloy formation. For the first time, we found that the electrochemical behavior of Al current collector in a LiBETI electrolyte is strikingly different from the conventional $LiPF_6$ electrolyte in the potential range of 0–5 V versus Li/Li^+, namely, significant inhibition of Li–Al alloy formation at 0 V versus Li/Li^+ and passivation with thin Al–F outer layer supported by Al–O inner layer at 5 V versus Li/Li^+. The surface chemistry of aluminum in a LiBETI system is discussed in relation to the film structure. Finally, we demonstrate that the Li–Al alloy inhibition character is applied to SnO_2 electrode to demonstrate feasibility of aluminum that works as a current collector for negative electrode in a LiBETI electrolyte.

2. Experimental

Pure aluminum foil (lithium battery grade, 20 μm thick) was cut into squares (10 × 40 mm^2) for polarization tests. Then, the aluminum specimen was washed with pure ethanol. Aluminum pouch cells were fabricated in an Ar-filled glove box. The electrochemical cells consisted of an aluminum specimen with an exposed area of 1 cm^2 as a working electrode and lithium metal as counter and reference electrodes separated by a porous polypropylene separator in a 1 M LiBETI (3M company) solution with an ethylene carbonate (EC)–dimethyl carbonate (DMC) mixture (1:1 ratio by volume) solvent.

Cathodic polarization was first applied from open circuit potential (OCP) to 0 V, and then the polarization progressed in an anodic direction up to 5 V with a sweeping rate of 10 mV s^{-1} at 40 °C. In scratch tests, a similar polarization was applied but with different destination potentials (0, 3, 4, and 5 V). When the potential reached the desired value, the surface of the aluminum specimen was scratched using a diamond tip at 100 rpm for a few seconds in an H-type cell [4,6,12]. After scratching the electrode surface, the current variation versus time was monitored for 300 s.

The polarized specimen was washed with a carbonate ester solvent and transferred to a vacuum chamber of a ToF-SIMS instrument (ULVAC-PHI TRIFT2000) at 10^{-9} Torr. During the analysis, the targets were bombarded by pulsed 15 keV Ga^+ beams (0.5 pA target current) for an area of 12 × 12 μm^2. For depth analysis, Ga^+ beams were applied in a direct mode over an area of 240 × 240 μm^2.

Tin(VI) oxide was adopted as an active material for a working electrode in the cell with LiBETI electrolyte and an aluminum current collector. The crystalline phase of commercially available nanocrystalline SnO_2 (<30 nm, Wako Chemicals) was characterized by powder x-ray diffraction (XRD; Rint-2000, Rigaku) analysis using Cu-Kα radiation. The particle morphology was observed using transmission electron microscopy (TEM; H-800, Hitachi). Fig. 1 shows the XRD pattern and TEM image for the nanocrystalline SnO_2 used in this study. For fabrication of composite electrodes, the SnO_2 powders were mixed with carbon black and polyacrylic acid or polyvinylidene fluoride (85:7.5:7.5) in *N*-methylpyrrolidinone. The obtained slurry was coated onto copper or aluminum foil and hot pressed at 120 °C. The electrodes were dried overnight at 120 °C in a vacuum prior to use. Cell tests were done with aluminum pouch cells using lithium metal as a counter electrode. The assembled cells were cycled between 0.25 V and 2 V by applying a constant current of 50 mA g^{-1} at 30 °C.

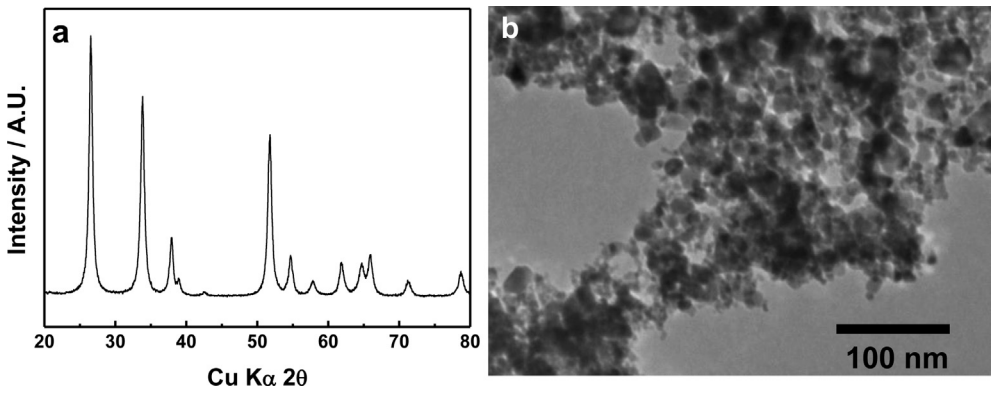

Fig. 1. (a) Powder XRD patterns of nanocrystalline SnO_2 and (b) corresponding bright-field TEM image.

3. Results and discussion

To understand the electrochemical stability of aluminum in a LiBETI electrolyte, an aluminum specimen was polarized over the potential range of 0–5 V in an EC-DMC solution of 1 M LiBETI (Fig. 2). During the cathodic polarization of the aluminum specimen from OCP (2.548 V), no apparent change in current was found up to 1.5 V. From 1.5 to 0 V a gradual increase was observed in cathodic current, which could result from reduction of the electrolyte, formation of a solid electrolytic interface, and under potential deposition of lithium. The current was maximized at 0 V where Li–Al alloy could form. Note that much lower cathodic current is observed in the LiBETI electrolyte (<20 μA cm^{-2}) than that in a $LiPF_6$ electrolyte as reported previously (<3 mA cm^{-2} [5]).

In both cases, the only difference is electrolytic salt for the above mentioned electrolytes. Although air-formed films (Al_2O_3/AlOOH) on the aluminum specimen might be reduced somehow, the oxide layer does not seem to be reduced effectively to aluminum metal in the LiBETI electrolyte. Assuming the air-formed layer is 10 nm thick Al_2O_3, the charge density necessary to reduce the whole oxide to metal was calculated to be 1.1×10^{-2} C cm^{-2}. By contrast, the measured charge density for the specimen from the OCP to 0 V was 2.3×10^{-3} C cm^{-2}, which is far lower than the calculated value. This result supports the hypothesis that the air-formed oxide layer is scarcely reduced in a LiBETI electrolyte. It is likely that the presence of less aggressive BETI anion, $(SO_2C_2F_5)_2N^-$), compared to F^- in $LiPF_6$, is a possible factor that does not lead to effective reduction of air-formed films.

To confirm that Li–Al formation is inhibited by an air-formed oxide layer, a naked aluminum surface was exposed to a LiBETI electrolyte at 0 V by means of *in situ* scratching. When the surface of the aluminum electrode was scratched, the resulting cathodic current abruptly increases (Fig. 3), indicating the formation of Li–Al alloy. An optical microscopy image clearly showed the formation of Li–Al alloy on the aluminum electrode (see, inset of Fig. 3). This result supports that air-formed surface layers keep its barrier ability against Li–Al alloy formation in a LiBETI system, although it cannot be retained in a $LiPF_6$ system. We reported similar findings in a LiBOB system [6].

The reverse reaction, the oxidation of deposited lithium, was seen during the anodic polarization (inset of Fig. 2), after which the resulting current was kept constant at a very low level to 3.5 V. Then, a gradual increase in anodic current was observed up to 5 V,

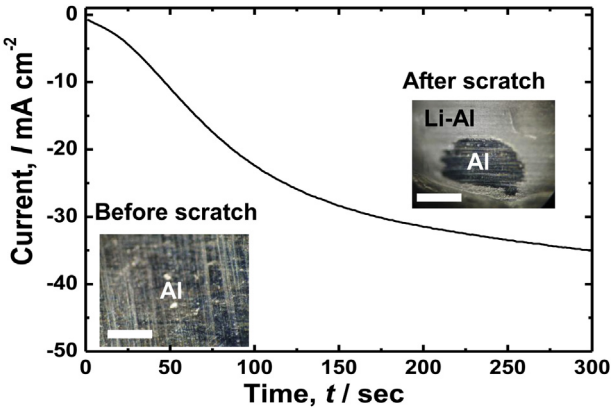

Fig. 3. *In-situ* scratch test at 0 V versus Li/Li^+ during cathodic polarization (optical microscopic images describes surfaces of the Al electrode before and after the scratch tests). Scale bar indicates 1 mm.

suggesting that either the aluminum specimen underwent further oxidation or the electrolyte was being decomposed at this potential. The reaction is irreversible, as indicated by the absence of cathodic peaks during the cathodic sweeping back to 2.5 V in the three consecutive cycles. As has been reported [9], aluminum does not suffer from severe corrosion in a LiBETI system over the potential range of 0–5 V. In order to understand whether an air-formed oxide layer just protects aluminum from corrosion like in case of Li–Al alloy formation or a protective film can be reproduced in a LiBETI electrolyte, scratch tests were carried out.

The surface of an aluminum specimen, whose potential has reached a given value starting from the OCP via 0 V, was scratched by a diamond tip to follow the current during anodic polarization in a LiBETI electrolyte (Fig. 4). At 3 V, where the anodic current density in Fig. 2 was quite low, the current decayed very fast and remained at a low level. Based on the thermodynamic consideration, aluminum metal can be oxidized to a trivalent Al-oxide at 1.4 V (−1.66 V versus SHE [13]). When the oxide layer was removed at 3 V, the naked surface would be immediately oxidized to form new films in the electrolyte. This, in turn, leads to a sharp decrease in current (Fig. 4). At 4 V, the transient was similar to the tendency observed at 3 V, showing a sharp decay followed by a relatively low level of current. At 5 V, the current was also lowered gradually, but

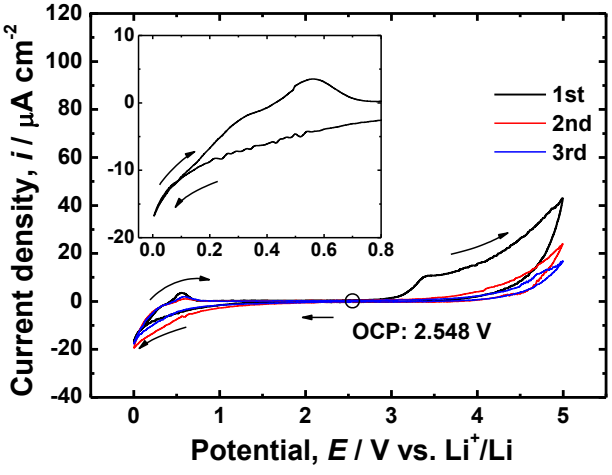

Fig. 2. Three consecutive cyclic voltammograms of Al foil polarized in a 1 M LiBETI – (EC-DMC) solution.

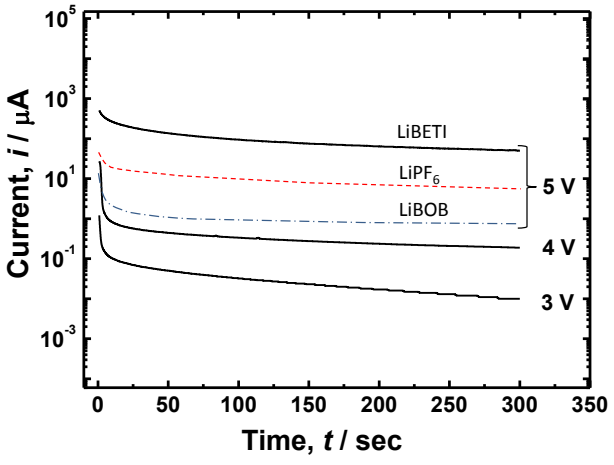

Fig. 4. Time and current (i–t) curves of Al foil after the scratching test at 3, 4, and 5 V versus Li/Li^+ polarized in a 1 M LiBETI – (EC-DMC) solution. Similar i-t curves in $LiPF_6$ [5] and LiBOB [6] systems are also drawn for comparison.

the magnitude of the current was much larger in comparison with the results at 5 V in $LiPF_6$ [5] and LiBOB [6] electrolytes. For example, the currents at 100 s after the scratch were 95 μA (LiBETI), 42 μA ($LiPF_6$) and 13 μA (LiBOB), respectively. The order is typical and would not be changed by the possible differences in the scratched area in each run. The result indicates that the passivation of aluminum in a LiBETI electrolyte is somewhat slower than in other types of electrolytes. In fact, the corrosion of aluminum in

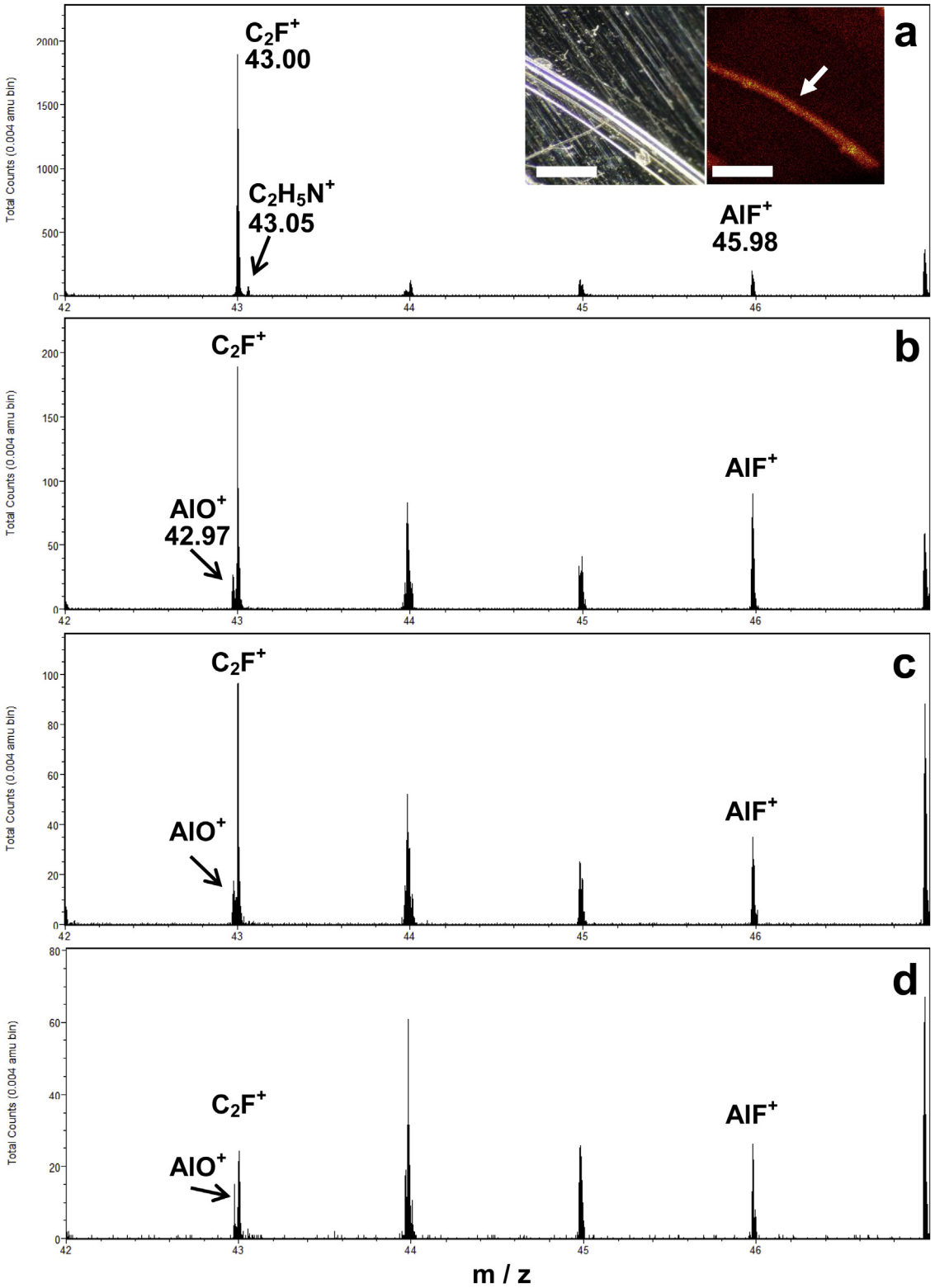

Fig. 5. ToF-SIMS spectra after the scratch test at 5 V versus Li/Li^+ for 300 s transient polarization; (a) as-received, Ga^+ sputtered for (b) 30 s, (c) 100 s, and (d) 1000 s. Inset in (a) presents the optical microscopic (left) and secondary-ion (Al^+) mapping images (right). The scale bar denotes 100 μm.

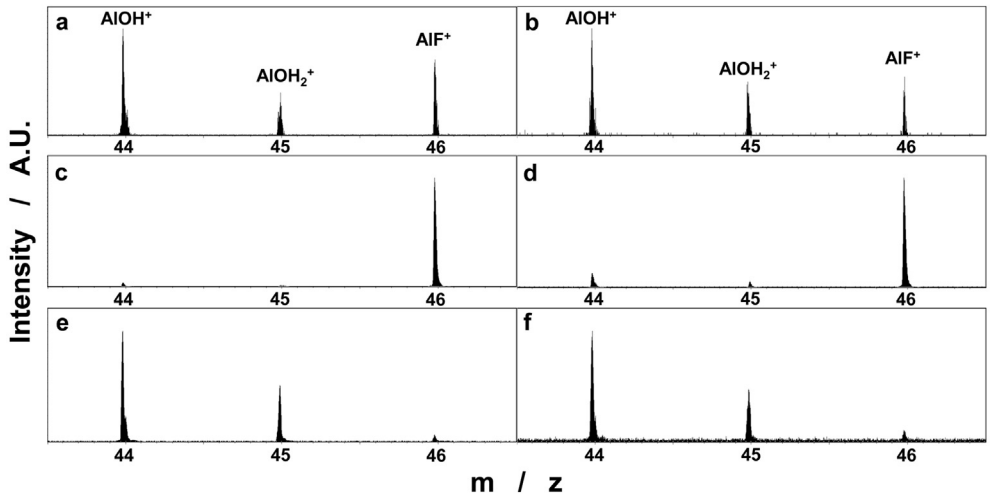

Fig. 6. ToF-SIMS spectra for the aluminum polarized at 5 V versus Li/Li^+ for 300 s in several electrolytes; containing 1 M LiBETI salt after sputtering (a) 30 s and (b) 1000 s; containing 1 M $LiPF_6$ salt after sputtering (c) 30 s and (d) 1000 s; 0.8 M LiBOB salt after sputtering (e) 30 s and (f) 1000 s.

imide-type electrolytes is known to be inhibited by the addition of $LiPF_6$ [3,10,14–17], which facilitates the formation of fluorinated layers on the outermost oxide layers. From the above results on the alloying and passivation behavior of aluminum, it is considered that films formed on aluminum in a LiBETI electrolyte differ from those formed in $LiPF_6$ [5] and LiBOB electrolytes [6].

After the *in situ* scratch at 5 V polarized for 300 s, the scratched surface was analyzed by Ga^+ ion beam onto the track ($12 \times 12\ \mu m^2$). The resulting secondary ion mapping (Al^+) image exhibited clear vestiges after the *in situ* scratch (inset of Fig. 5a). The as-scratched part (arrow marked) showed a relatively strong signal of C_2F^+ fragment ($m/z = 43.00$), which originated from the salt decomposition at 5 V (Fig. 5a). A weak AlF^+ ($m/z = 45.98$) fragment was detected, but oxide fragment, AlO^+, was not observed. By etching with the Ga^+ ion beam for 30 s (Fig. 5b), the relative intensity of the C_2F^+ fragment markedly decreased, indicating that the C–F complex layer is not thick and dense. Meanwhile, The weak AlO^+ ($m/z = 42.97$) fragment appeared in the spectra. Fragment ions that stemmed from the possible compounds between the aluminum cation and BETI anion like $[AlN(SO_2C_2F_5)_2]^+$ were not detected even on the outermost surface, because the LiBETI salt was probably decomposed to several moieties containing N, S, O, and F elements.

Fig. 6 also includes the results of similar experiments in $LiPF_6$ and LiBOB electrolytes for comparison. Earlier study by Morita et al. [7,10] elucidated that the surface of Al electrode was completely passivated by AlF_3 (and $Al(OH)_3$, Al_2O_3) in $LiPF_6$/EC-DMC solution. Also, the addition of $LiPF_6$ to the imide-salt solutions suppresses the Al corrosion through formation of a fluoride (AlF_3)-rich film on the Al surface. In LiBETI electrolyte (Fig. 6(a)), AlF^+ ($m/z = 45.98$) fragment was detected, but more intense was hydroxide fragment, $AlOH^+$($m/z = 43.98$). The relative intensity of $AlOH^+$ against AlF^+ increased as sputtering progressed (Fig. 6(b)), which is similar to the case of films formed in a $LiPF_6$ electrolyte (Fig. 6(c) and (d)). In a $LiPF_6$ electrolyte, films formed on aluminum were more deeply covered with an AlF_3 layer (Fig. 6(c)): the AlF^+ peak were still dominant even after 1000 s sputtering (Fig. 6(d)). In a LiBOB electrolyte, which is free from fluorine element, surface films were composed of oxide/hydroxide even after the 1000 s sputtering (Fig. 6(e) end (f)), by which Al–Li alloy formation was effectively suppressed at 0 V [6]. Surface films formed in the presence of LiBETI, as well as $LiPF_6$, are composed of two layers, namely an Al–F (AlF_3) outer layer and an Al–O (Al_2O_3/AlOOH) inner layer. However, a LiBETI salt is known to have good durability against moisture. Thus, the reaction that takes place in a $LiPF_6$ system

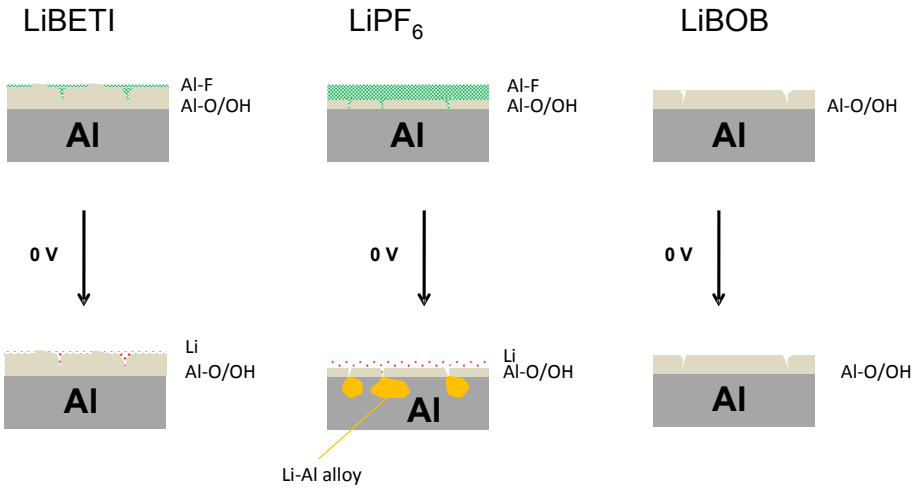

Fig. 7. Schematic drawing of the effect of electrolyte on the structure of surface films and Li–Al alloy formation process on aluminum.

($LiPF_6 + H_2O \rightarrow LiF + 2HF + POF_3$) does not readily occur with BETI anions, implying little formation of HF during anodic polarization. The fluoride layer is much thinner in the LiBETI electrolyte, and the thicker oxide/hydroxide layers are likely to protect the aluminum bulk from being alloyed with lithium at 0 V and to maintain a passive state up to 5 V. The idea as mentioned above is schematically illustrated in Fig. 7.

So far, alloying and passivation behavior has been discussed for aluminum just exposed to electrolytes. However, current collectors are always used together with active materials, conducting materials (carbon) and binders; thus, a composite was applied on a current collector. Since the added substances may affect alloying and passivation, an aluminum current collector was tested with these composites varying active materials such as graphite and nano-sized SnO_2, and binders like PVDF and PAA in a LiBETI electrolyte (Fig. 8). In the case of graphite bound to aluminum using PVDF binder, Li^+ ion intercalation into the graphite did not precede alloy formation (Fig. 8a). A long plateau at around 0.25 V is an indication of the Li–Al alloy formation process. For this reason, a fluorine-free binder, PAA, was chosen. By contrast to what was anticipated, we found the same long plateau, which appeared for the PVDF binder (Fig. 8b). The results strongly suggest that Li–Al formation is accelerated by the contact of aluminum with graphite even in a LiBETI electrolyte.

Another active material of nanocrystalline SnO_2 was used with the fluorine-free binder, PAA, and the lower cut-off voltage was raised to 0.25 V. For a copper current collector, the nano-SnO_2 exhibited typical charge and discharge behavior for 10 cycles (Fig. 9a). Preliminary screening tests for choice of active materials (SnO_2, Si, SiO_x, Co_3O_4, and NiO) indicated that SnO_2 is one of the suitable materials with Al current collector in LiBETI electrolyte. When aluminum foil was substituted for copper as a current collector, no differences in the capacity and curve profiles were observed during cycling (Fig. 9b). This fact suggests that the alloying of aluminum with lithium is inconsiderable during the cycling. The delivered reversible capacity is approximately 460 mAh (g-oxide)$^{-1}$ in the voltage range of 0.25–2 V. It should be noted that the PVDF binder containing nano-SnO_2 electrode resulted in alloy formation below 0.3 V (Fig. 9c), which can

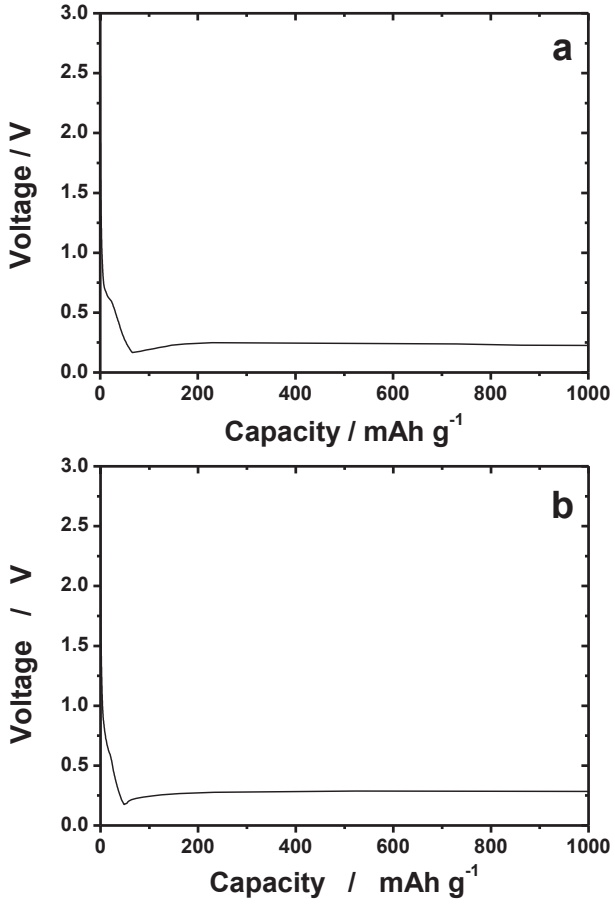

Fig. 8. The first charge curves of graphite on an aluminum current collector using (a) PVDF and (b) PAA binders in a 1 M LiBETI – (EC-DMC) solution.

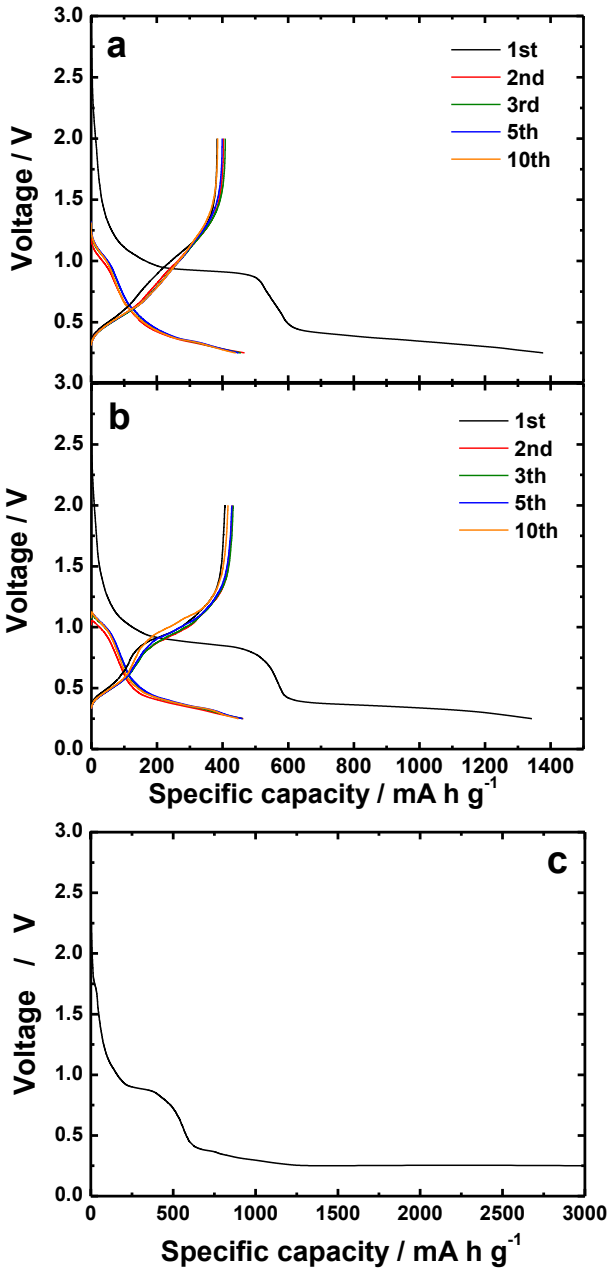

Fig. 9. Continuous charge and discharge curves of nano-SnO_2 coated on (a) Cu and (b) Al foil cycled in a 1 M LiBETI – (EC-DMC) solution. The binder used was PAA for the above electrodes. (c) The first charge curve of nano-SnO_2 coated on Al foil in a 1 M LiBETI – (EC-DMC) solution. The binder used was PVDF for the electrode fabrication.

probably be ascribed to the presence of fluorine in the PVDF binder. The above results demonstrate the feasibility of Al current collector for negative electrode application in LiBETI electrolyte. Although the price of LiBETI salt is still expensive, mass production would reduce the salt price similar to $LiPF_6$ salt level. It is also anticipated that the combination with SnO_2 and Al instead of Cu current collector is applicable to large-scale cost effective energy storage area.

4. Conclusion

The present study showed that the alloying behavior of aluminum with lithium was affected by the stability of the oxide layer on electrochemical reduction at 0 V. Aluminum in a $LiPF_6$-containing electrolyte, where its surface oxide layer was deeply fluorinated, was easily alloyed with lithium, whereas it was significantly inhibited in a LiBETI-containing electrolyte. ToF-SIMS analysis indicated less fluorinated nature of oxide layers on aluminum in a LiBETI electrolyte. However, aluminum in contact with graphite was alloyed even in a LiBETI electrolyte, probably because the graphite facilitates electrochemical reduction of the oxide layers on aluminum. Eventually, the nano-sized SnO_2 powders on an aluminum current collector exhibited comparable capacity to that with a conventional copper current collector in the range of 0.25–2 V only when the fluorine-free polyacrylic acid was used as a binder. Aluminum was stable up to 5 V in a LiBETI electrolyte even after scratching. Meanwhile, the repassivation kinetics was somewhat slower as compared to a $LiPF_6$ salt-containing electrolyte. It can be concluded that a LiBETI electrolyte enlarges the applicability of an aluminum current collector in rechargeable lithium batteries with a wide potential window, not only for a positive electrode, but also for a negative electrode.

Acknowledgments

The authors thank the 3M company (Mr. Segawa) for providing the lithium imide salt. This study was supported in part by a grant from the National Research Foundation of Korea funded by the Korean government (MEST) (NRF-2009-C1AAA001-0093307). This work was also supported by the Secondary Battery R&D Program for Leading Green Industry of MKE/KEIT [10041094].

References

[1] K. Kanamura, T. Okagawa, Z. Takehara, J. Power Sources 57 (1995) 119–123.
[2] J.W. Braithwaite, A. Gonzales, G. Nagasubramanian, S.J. . Lucero, D.E. Peebles, J.A. Ohlhausen, W.R. Cieslak, J. Electrochem. Soc. 146 (1999) 448–456.
[3] S.S. Zhang, T.R. Jow, J. Power Sources 109 (2002) 458–464.
[4] T.C. Hyams, J. Go, T.M. Devine, J. Electrochem. Soc. 154 (2007) C390–C396.
[5] S.-T. Myung, Y. Sasaki, S. Sakurada, Y.-K. Sun, H. Yashiro, Electrochim. Acta 55 (2009) 288–297.
[6] S.-T. Myung, H. Natsui, Y.-K. Sun, H. Yashiro, J. Power Sources 195 (2010) 8297–8301.
[7] M. Morita, T. Shibata, N. Yoshimoto, M. Ishikawa, J. Power Sources 199–121 (2003) 784–788.
[8] S.-W. Song, T.J. Richardson, G.V. Zhuang, T.M. Devine, J.W. Evans, Electrochim. Acta 49 (2004) 1483–1490.
[9] L.J. Krause, W. Lamanna, J. Summerfield, M. Engle, G. Korba, R. Loch, R. Atanasoski, J. Power Sources 68 (1997) 320–325.
[10] M. Morita, T. Shibata, N. Yoshimoto, M. Ishikawa, Electrochim. Acta 47 (2002) 2787–2793.
[11] D.D. Censo, I. Exnar, M. Graetzel, Electrochem. Commun. 7 (2005) 1000–1006.
[12] S.-T. Myung, Y. Sasaki, T. Saito, Y.-K. Sun, H. Yashiro, Electrochim. Acta 54 (2009) 5804–5812.
[13] M.C. Ball, A.H. Norbury, Physical Data for Inorganic Chemists, Longman, London, 1974, p. 118.
[14] X. Wang, E. Yasukawa, S. Mori, Electrochim. Acta 45 (2000) 2677–2684.
[15] T. Nakajima, M. Mori, V. Gupta, Y. Ohzawa, H. Iwata, Solid State Sci. 4 (2002) 1385–1394.
[16] H. Yang, K. Kwon, T.M. Devine, J.W. Evans, J. Electrochem. Soc. 147 (2000) 4399–4407.
[17] S.-T. Myung, H. Yashiro, Y.-K. Sun, J. Mater. Chem. 21 (2011) 9891–9911.